Radiation Measurements 124 (2019) 40–47

Contents lists available at ScienceDirect

Radiation Measurements

journal homepage: www.elsevier.com/locate/radmeas

Thermoluminescence governed by the Auger-recombination process

J.L. Lawless[a], R. Chen[b,*], V. Pagonis[c]

[a] Redwood Scientific Incorporated, Pacifica, CA, 94044-4300, USA
[b] Raymond and Beverly Sackler School of Physics and Astronomy, Tel Aviv University, Tel Aviv, 69978, Israel
[c] Physics Department, McDaniel College, Westminster, MD, 21157, USA

ARTICLE INFO

Keywords:
Thermoluminescence (TL)
Auger recombination
Third-order kinetics
Superlinearity
High frequency factor

ABSTRACT

In the present work, we study the possibility that a thermoluminescence (TL) peak is governed by the effect of Auger recombination, an effect which has been considered for other luminescence phenomena. In Auger recombination in the form of interest here, two conduction-band electrons are involved in the recombination of one of them with a hole in a center. The two electrons collide in the presence of the center, one loses energy and recombines, yielding a TL photon, and the other gains energy and speeds away. As mentioned with regard to other luminescence phenomena, in this case, in the set of differential equations governing this process, a term proportional to the square of the free-electron concentration should be included in analogy to the law of mass action. The relevant set of simultaneous differential equations has been solved numerically for feasible sets of parameters. The results yield a relatively narrow TL peak which is somewhat asymmetric, with the fall-off half being larger than the low-temperature half. Under appropriate conditions, the set of equations is shown to reduce to an approximate third-order kinetic equation, the solution of which has a very similar symmetry. The third-order approximate curve has an effective activation energy which is twice as large as the original. Such asymmetric peaks have been described in the literature. Also, when using standard peak-shape methods for evaluating the effective activation energy and frequency factor very high values of these magnitudes have been found due to the narrowness of the simulated peak. This model may explain the occurrence of such TL peaks previously reported in the literature. Also is discussed the possible concurrent regular Randall-Wilkins recombination and Auger recombination within the one-trap-one-recombination center (OTOR) model. In another version of the model, an additional thermally disconnected trap is considered. With certain sets of parameters, the simulations yield a cubic dependence of TL intensity on the excitation dose, an effect previously reported in some materials.

1. Introduction

In the study of luminescence and other phenomena in solids, the possibility of the occurrence of Auger recombination should be considered. Auger recombination occurs in different ways. The one of interest for thermoluminescence (TL) has to do with two electrons colliding with a center. Assuming that the center contains one hole, which is considered to be the normal case, one of the electrons recombines with the hole in the center. The other electron remains free and carries away the excess energy. In other words, in Auger recombination, two free electrons collide with a center. One electron loses energy and recombines whereas the other gains some energy and speeds away. When this is the case, the equations governing the processes during excitation, relaxation and heating change. This change is associated with a different behavior of some aspects of TL than is expected in the conventional (Randall-Wilkins) one-trap-one-center (OTOR) model.

The possibility that Auger recombination takes part in different aspects of luminescence has been discussed in the literature. Łożykowski et al. (1975) described an anti-Stokes emission in the electroluminescence of ZnSe-ZnTe diodes and explained it as being due to Auger recombination. Auston et al. (1975) discussed the transient high-density electron-hole plasmas in germanium. The authors used a third-order kinetic equation and stated that the cubic dependence of the recombination rate arises from the three-body character of the Auger process, whereby an electron recombines with a hole, and the excess energy is transferred to another electron as kinetic energy. The Auger constant they use has units of $cm^6 s^{-1}$ as discussed further below. Benz and Conradt (1977) have communicated on luminescence resulting from Auger recombination in n-type and p-type GaAs and GaSb. They have reported on Auger constants between 10^{-25} and 10^{-31} $cm^6 s^{-1}$. Pilkuhn (1979) has discussed non-radiative recombination and luminescence attributed to Auger transitions in silicon. Ghanassi et al.

* Corresponding author.
E-mail address: chenr@tauex.tau.ac.il (R. Chen).

https://doi.org/10.1016/j.radmeas.2019.03.002
Received 2 October 2018; Received in revised form 14 January 2019; Accepted 5 March 2019
Available online 08 March 2019
1350-4487/

(1993) have reported on the optical properties of semiconductor-doped glasses (SDG) and confirmed the role of Auger recombination in the results. Aytac et al. (2016) have studied some optical properties of InAs/InAsSb superlattices and reported Auger coefficients of $\sim 10^{-25}$ $cm^6 s^{-1}$. Theoretical work on different kinds of the Auger effect which bears some relevance to the present case have been given by Sheinkman (1964), Tolpygo et al. (1965, 1974) and by Vorobev et al. (1984).

The possibility that Auger recombination may be involved in the TL process has been mentioned in the literature. Tuan et al. (1972) interpreted their results of TL in X-ray irradiated KI crystals at temperatures in the range of 90–180 K in terms of the Auger process. Böhm and Scharmann (1981) and Scharmann and Böhm (1993) discussed the occurrence of TL governed by the Auger process. The possible occurrence of Auger thermoluminescence has been mentioned by McKeever (1985) but he has stated that although Auger collisions are a feasible TL process, no experimental evidence had existed to indicate that they might be important in TL processes. Oster and Haddad (2003) have described "exotic cases" of energy transfer in solids which include TL associated with the Auger recombination.

2. The model

As pointed out above, the Auger recombination of the kind relevant to the present work includes the participation of two electrons and one hole. In full analogy to the law of mass action, dealing with the rate equations of chemical reactions (Guldberg and Waage, 1864; Lund, 1965; Hinkley and Tsokos, 1974; Baird, 1999; Ferner and Aronson, 2016), the relevant term for the simultaneous recombination of two electrons should be proportional to n_c^2 where n_c (cm^{-3}) is the concentration of free electrons but linear with m (cm^{-3}), the concentration of the holes in centers. Therefore, the term mn_c^2 will appear in the kinetic equations. In this work, we will consider two versions of the Auger model. One is a one-trap-one-recombination-center (OTOR) model with Auger recombination and the other includes an additional, thermally disconnected trap, which acts as a trapping competitor. It should be noted that in TL materials, it is very rare to find a crystal with only one type of trapping state, thus the addition of at least one competing trap seems quite natural.

The model relevant to the latter case is depicted in Fig. 1. The transitions taking place both during excitation and heating are shown. The active trap is shown with concentration of N_1 (cm^{-3}), instantaneous occupancy of n_1 (cm^{-3}), activation energy E_1 (eV) and frequency factor s_1 (cm^{-3}). The competing trap has concentration N_2 (cm^{-3}), instantaneous occupancy n_2 (cm^{-3}), activation energy of E_2 (eV) and frequency factor s_2 (s^{-1}). We will assume here that E_2 is significantly larger than E_1 which makes E_2 a disconnected trap in the range of occurrence of the TL peak associated with E_1. M (cm^{-3}) is the concentration of hole centers and m (cm^{-3}) its instantaneous occupancy. The rate of producing electron-hole pairs by irradiation in the conduction and valence band respectively is X ($cm^{-3}s^{-1}$), which is proportional to the dose rate of excitation. A_1 (cm^3s^{-1}) and A_2 (cm^3s^{-1}) are the retrapping-probability coefficients into N_1 and N_2, respectively. B (cm^3s^{-1}) is the trapping probability coefficient of free holes into the center during excitation. A_a (cm^6s^{-1}) is the Auger-recombination probability coefficient which, as pointed out above has different dimensions than the other mentioned probability coefficients. n_c (cm^{-3}) and n_v (cm^{-3}) are the instantaneous concentrations of free electrons and free holes, respectively.

2.1. Auger recombination within the OTOR model

Let us start by the simple case where no competing trap is considered. In this case, at the end of irradiation, the concentrations of electrons in traps and holes in centers will be the same, and we can choose these concentrations, $n_0 = m_0$, quite arbitrarily. We can skip the stages of excitation and relaxation in the simulation (see below the more general case) and solve the equations only for the heating stage. Also, we can remove at this stage the subscript "1″ in this case since we are considering only one trap.

The set of equations governing the process during heating is

$$\frac{dn}{dt} = A\cdot(N-n)\cdot n_c - s\cdot n\cdot\exp(-E/kT), \tag{1}$$

$$\frac{dn_c}{dt} = -A\cdot(N-n)\cdot n_c - A_a\cdot m\cdot n_c^2 + s\cdot n\cdot\exp(-E/kT), \tag{2}$$

$$I = -\frac{dm}{dt} = A_a\cdot m\cdot n_c^2, \tag{3}$$

where k ($eV\cdot K^{-1}$) is the Boltzmann constant, T (K) is the absolute temperature and t (s) is time. The main new point in these equations is the occurrence of the mn_c^2 term in Eqs. (2) and (3). The TL intensity is I ($cm^{-3}s^{-1}$) given in Eq. (3); a dimensional constant changing the units into intensity units could be added here. The reason why A_a has units of cm^6s^{-1} is obvious from Eqs. (2) and (3).

Let us make the usual quasi-steady assumption. The free electron lifetime is short compared to the heating times, then the rate of generation of free electrons must be approximately equal to the rate of recombination of free electrons, and Eq. (2) reduces to

$$A_a m n_c^2 + A(N-n)n_c = sn\exp(-E/kT). \tag{4}$$

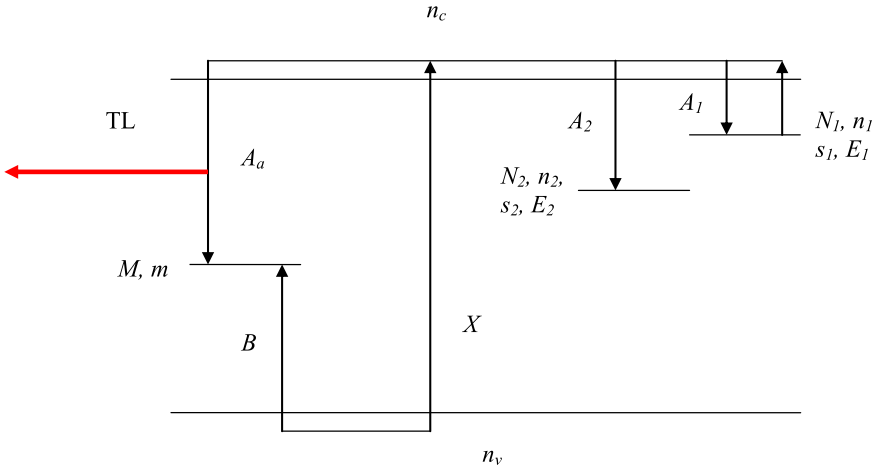

Fig. 1. Energy level diagram of the model with an active trap N_1 and a competing trap N_2, and a hole recombination center M. The meaning of the relevant parameters is given in the text.

Solving the quadratic equation in n_c yields

$$n_c = \frac{-A(N-n) \pm \sqrt{A^2(N-n)^2 + 4A_a mns\exp(-E/kT)}}{2A_a m}. \quad (5)$$

Let us assume that the dose is low enough so that $n << N$ and $\frac{4A_a s\exp(-E/kT)}{A^2N^2}mn << 1$. Also, since we are dealing with the one-trap-one recombination center (OTOR), we can assume that $m \approx n$. we thus have

$$n_c = \frac{ms\exp(-E/kT)}{AN}. \quad (6)$$

Inserting in Eq. (3), we get

$$I = -\frac{dm}{dt} = \left(\frac{A_a s^2}{A^2N^2}\right)\cdot m^3\cdot\exp(-2E/kT). \quad (7)$$

The solution of Eq. (7) can be given explicitly as

$$I(T) = C\cdot m_0^3\cdot\exp(-2E/kT)/\left[1 + (2C\cdot m_0^2/\beta)\int_{T_0}^{T}\exp(-2E/kT')dT'\right]^{3/2}, \quad (8)$$

where $C = A_a s^2/(AN)^2$.

The third-order equation is the result of the center m and trap n emptying at nearly the same rate and it is peculiar to OTOR. Note that the effective activation energy is expected here to be $\sim 2E$. Also, the pre-exponential term in Eq. (7) has the same dimension as A_a. In the cases reported below, the numerical solution of Eqs. (1)–(3) will be compared to that of Eq. (8) for relevant sets of the parameters. Note that, as mentioned above, Auston et al. (1975) suggested that cubic dependence of the recombination rate arises from the three-body character of the Auger process.

2.2. Auger recombination with a competing trapping state

In the case of Auger recombination within the OTOR model, we could assume that at the end of irradiation followed by relaxation the concentrations of trapped electrons and holes are the same, and rather arbitrary values of the initial concentrations $n_0 = m_0$ could be chosen. With this choice, we could solve the simultaneous equations (1)–(3) with a certain heating function. This is not the case for the model with additional trapping state. Here, we must consider the excitation and relaxation stages which, for a given set of parameters determine the distribution of electrons between the two traps following excitation and relaxation, prior to the beginning of the heating stage. The set of coupled differential equations for the excitation stage is

$$\frac{dn_1}{dt} = A_1\cdot(N_1 - n_1)\cdot n_c - s_1\cdot n_1\cdot\exp(-E_1/kT), \quad (9)$$

$$\frac{dn_2}{dt} = A_2\cdot(N_2 - n_2)\cdot n_c - s_2\cdot n_2\cdot\exp(-E_2/kT), \quad (10)$$

$$\frac{dn_c}{dt} = X - A_1\cdot(N_1 - n_1)\cdot n_c - A_2\cdot(N_2 - n_2)\cdot n_c - A_a\cdot m\cdot n_c^2 + s_1\cdot n_1 \cdot\exp(-E_1/kT) + s_2\cdot n_2\cdot\exp(-E_2/kT), \quad (11)$$

$$\frac{dm}{dt} = B\cdot(M - m)\cdot n_v - A_a\cdot m\cdot n_c^2, \quad (12)$$

$$\frac{dn_v}{dt} = X - B\cdot(M - m)\cdot n_v, \quad (13)$$

where the parameters are explained above with regard to Fig. 1; X ($cm^{-3}s^{-1}$) is the rate of production of electron-hole pairs by the irradiation, proportional to the dose rate. As pointed out above, we assume that E_2 is relatively large and consequently, the term $s_2n_2\exp(-E_2/kT)$ appearing in Eqs. (10) and (11) is negligibly small. Of course, heating the sample to much higher temperatures will release electrons from the deeper trap which may result in the occurrence of another, regular, TL peak. For a chosen set of relevant parameters, the equations are solved numerically for a certain length of time t_D (s). The total dose is represented by $D = X\cdot t_D$ (cm^{-3}), the total concentration of produced electron-hole pairs, proportional to the total applied dose. Following the simulation of the excitation, a relaxation period is simulated. The final values of the occupancies in the excitation stage are used as initial values for the relaxation. The excitation rate X is now set to zero and the process of solving the equations continues until n_c and n_v decrease to practically zero. The final values of the concentration functions are used as initial values to the next stage of heating. At this stage, the temperature is raised linearly at a rate of β (K/s), i.e., a heating function $T = T_0 + \beta t$ is used where T_0 is the initial temperature. Note that at this stage, $n_v \equiv 0$ and $X \equiv 0$, and therefore, Eq. (13) may be removed and Eqs. (9-12) be solved numerically. Obviously, like before, the emission of TL is associated with the term $A_a m n_c^2$ during heating.

2.3. Auger recombination along with Randall-Wilkins (RW) recombination

The possible occurrence of the Auger recombination does not exclude the appearance in parallel of the "regular" Randall-Wilkins (RW) like recombination. Referring to Fig. 1, in parallel to the radiative transition associated with the Auger recombination probability recombination A_a (cm^6s^{-1}), the other transition will have a probability coefficient A_m (cm^3s^{-1}) and it may be radiative as well. For the sake of simplicity, we consider here the OTOR case only, namely, without the thermally disconnected trap. The set of equations (1)–(3) transforms into

$$\frac{dn}{dt} = A\cdot(N - n)\cdot n_c - s\cdot n\cdot\exp(-E/kT), \quad (14)$$

$$\frac{dn_c}{dt} = -A\cdot(N - n) - A_a\cdot m\cdot n_c^2 + s\cdot n\cdot\exp(-E/kT) - A_m\cdot m\cdot n_c, \quad (15)$$

$$\frac{dm}{dt} = -A_a\cdot m\cdot n_c^2 - A_m\cdot m\cdot n_c, \quad (16)$$

where the term associated with the RW-like recombination has been subtracted from the right-hand side of Eqs. (2) and (3). The light emission is associated with either $A_a m n_c^2$ or with $A_m m n_c$ or with some weighted sum of these magnitudes. Some examples of simulations with this set of equations are given below.

3. Numerical results

The differential equations are solved numerically by the MATLAB ode15s solver, designed to handle stiff sets of equations. Fig. 2 shows an example of a solution of the simultaneous differential equations (1)–(3) (curve a) and the approximation given by Eq. (8) (curve b). The parameters chosen have been $E = 0.8$ eV; $s = 10^{13}\,s^{-1}$; $A_a = 10^{-25}\,cm^6s^{-1}$; $A = 10^{-10}\,cm^3s^{-1}$; $N = 10^{17}\,cm^{-3}$, $n_0 = m_0 = 10^{15}\,cm^{-3}$; the heating rate has been $\beta = 1$ K/s. The two peaks look very similar with the third-order approximation being slightly higher, by $\sim$5%. The symmetry factor usually used to follow the order of kinetics is in both curves $\mu_g = 0.56$. It should be noted that for first-order peaks, the typical value of the symmetry factor is $\mu_g \sim 0.42$, and for second order it is $\mu_g \sim 0.52$ (see Chen, 1969). Peaks with higher values of the symmetry factor have been reported in the literature, as mentioned in the Discussion section below. The simulated and approximate peaks have been analyzed using the peak-shape method given by Chen (1969). The results for curve (a) are; $T_m = 313.8$ K; $E_{eff} = 1.40$ eV; $s_{eff} = 5.8\cdot10^{21}\ s^{-1}$. For curve (b) $T_m = 313$ K; $E_{eff} = 1.43$ eV; $s_{eff} = 1.7\cdot10^{22}\ s^{-1}$. The values of the effective activation energies are $\sim$12% lower than the expected $2E$; the possible reason will be discussed below. Also will be discussed the very high value of the effective frequency factor s_{eff}.

As pointed out above, in real crystals, there is usually more than one trap. As an example of this situation, we have simulated TL peaks with

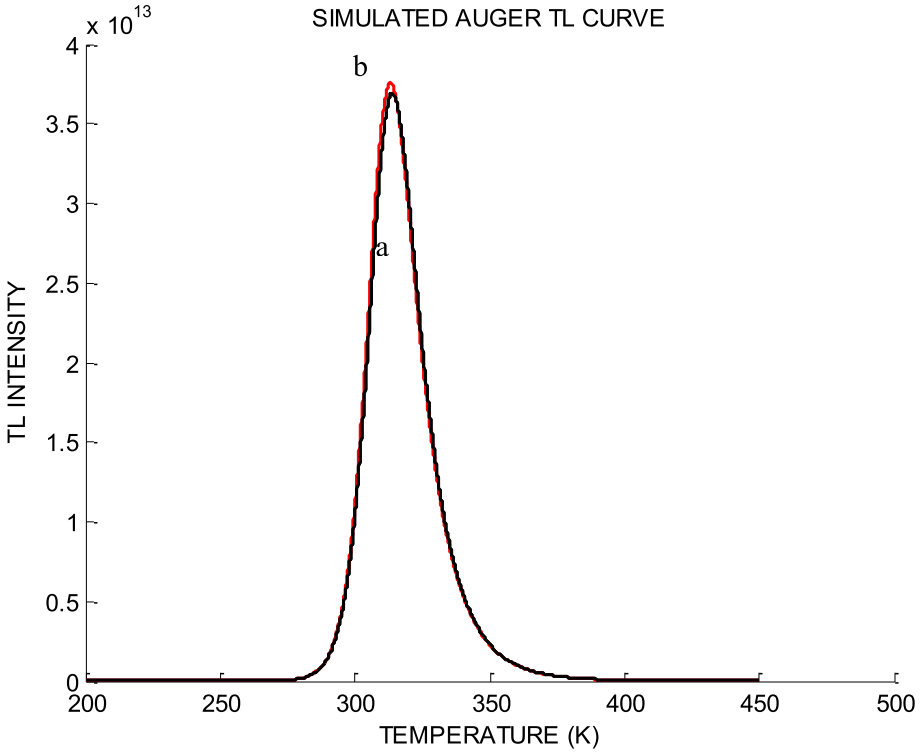

Fig. 2. Comparison of the numerical solution of the "pure" Auger-recombination simultaneous Eqs. (1)–(3) with Eq. (8), the solution of the third-order Eq. (7), with the same parameters. The set of parameters used is given in the text. Curve (a), the black line, depicts the solution of the simultaneous equations (1)–(3) and curve (b), the red line, shows the solution given in Eq. (8) with the same parameters. (For interpretation of the references to colour in this figure legend, the reader is referred to the Web version of this article.)

Auger recombination in the presence of a deep thermally disconnected competing trap, a situation described by Eqs. (9-13). The set of parameters chosen for this simulation has been (see Fig. 1) the following: $B = 10^{-11}$ cm^3s^{-1}; $A_1 = 10^{-12}$ cm^3s^{-1}; $A_2 = 10^{-11} cm^3s^{-1}$ $A_a = 10^{-25} cm^6s^{-1}$; $s_1 = 10^{12}$ s^{-1}; $s_2 = 10^{12}$ s^{-1}; $E_1 = 1.0$ eV; $E_2 = 2.5$ eV; $N_1 = 10^{17}\,cm^{-3}$; $N_2 = 10^{17}\,cm^{-3}$; $M = 10^{16}\,cm^{-3}$. The dose rate has been $X = 10^{15}\,cm^{-3}s^{-1}$ and the time of irradiation changed between 0.25 and 16 s, thus the total dose varied between $2.5 \times 10^{14}\,cm^{-3}$ and $1.6 \times 10^{16}\,cm^{-3}$. It should be noted that exactly the same results were found when the time of excitation was kept constant and the dose rate varied. An example of the results is shown in Fig. 3 for three excitation doses, (a) $10^{15}\,cm^{-3}$; (b) $2 \times 10^{15}\,cm^{-3}$; (c) $4 \times 10^{15}\,cm^{-3}$. The resulting TL peak looks like a pure first-order curve with a symmetry factor of 0.429, the same for all doses of excitation.

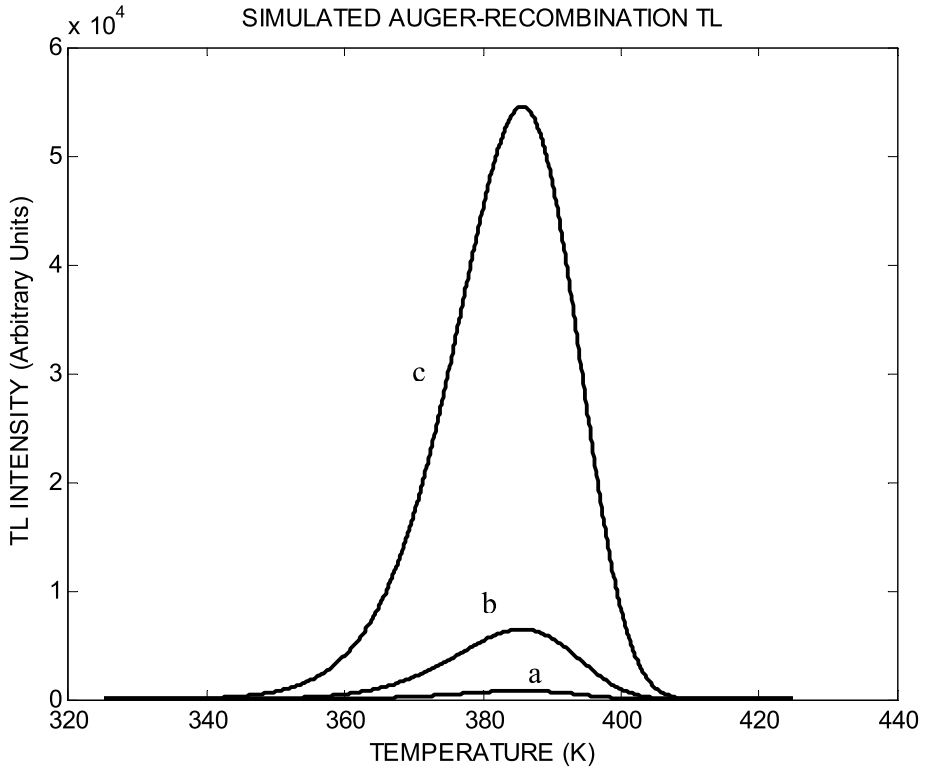

Fig. 3. Simulated glow peak using the Auger-recombination model with a thermally disconnected competitor. The set of parameters is given in the text. The excitation doses are: (a) $D = 10^{15}\,cm^{-3}$; (b) $D = 2 \times 10^{15}\,cm^{-3}$; (c) $D = 4 \times 10^{15}\,cm^{-3}$.

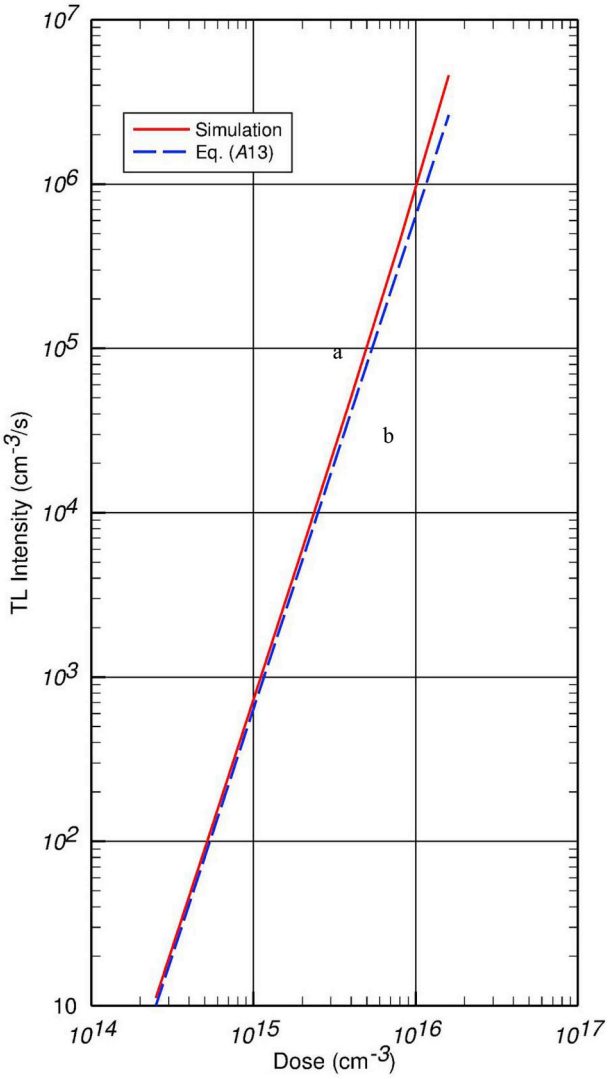

Fig. 4. Dependence of the maximum TL intensity on the dose on a log-log scale using the Auger recombination with the participation of a deep disconnected competitor. Curve (a) shows the results of the simulations and curve (b) depicts the approximate solution given by Eq. (*A*13).

This point will be discussed below. It should be noted, however, that this first-order looking peak does not have the original E and s effective values. Using the peak shape method, we found $E_{eff} = 1.52$ eV and $s_{eff} = 9.3 \times 10^{18}$ s^{-1}. This shows that although the peak has a shape of pure first-order curve, the effective activation energy and frequency factor have very high values related to the Auger-recombination effect. The peak's maximum-intensity strong dependence on the dose is seen in Fig. 4. The results are shown on a log-log scale where a nearly straight line with a slope of 3 is seen, meaning that a D^3 dose dependence takes place. It should be noted that the accumulated occupancies of traps and centers at the end of excitation and relaxation have been recorded as a function of the excitation dose and found to be linear. For an analytical approximate proof of this interesting result, see the Appendix. Curve (a) of Fig. 4 presents the results of the simulations whereas curve (b) shows the approximate dose dependence using the analytical expression developed in the Appendix. It is worth mentioning that the range of doses used for Fig. 4 is significantly broader than the three examples given in Fig. 3.

We report here two examples of simulations of the set of equations (14-16), where both Auger and RW-like recombinations take part in the process, one with relatively strong retrapping and one with weak retrapping. Fig. 5 depicts the results with the following set of parameters: $E = 1.0$ eV; $s = 10^{13}$ s^{-1}; $\beta = 1$ K/s; $A_a = 10^{-25}$ cm^{6}s^{-1}; $A_n = 10^{-15}$ cm^{3}s^{-1}; $A_m = 3 \times 10^{-14}$ cm^{3}s^{-1}; $N = 10^{17}$ cm^{-3}, $n_0 = m_0 = 10^{14}$ cm^{-3}. The three curves show the Auger recombination emission, the "normal" RW emission and also the concentration of free electrons, n_c, as a function of temperature. Note that this situation may be considered, as far as the RW-like emission is concerned, a strong retrapping case. The relevant magnitudes compared here are $A_m m$ and $A_n(N\text{-}n)$. At the outset, when $n_0 = m_0 = 10^{14}$ cm^{-3}, $A_m m_0 = 3 \times 10^{-14} \times 10^{14} = 3$ s^{-1} and retrapping dominates since $A(N\text{-}n_0) = 10^{-15} \times (10^{17}\text{-}10^{14}) \sim 100$ s^{-1}. The analysis of the Auger peak yields $\mu_g = 0.55$, $E_{eff} = 1.61$ eV and $s_{eff} = 8.5 \times 10^{19}$ s^{-1}, rather similar to that of the pure Auger-recombination peak. The analysis of the RW peak shows $\mu_g = 0.504$, $E_{eff} = 1.15$ eV and $s_{eff} = 1 \times 10^{14}$ s^{-1}.

The simulations leading to the results in Fig. 6 are different only in the value of the retrapping probability coefficient A which is significantly smaller here, $A = 10^{-17}$ cm^{3}s^{-1}. The Auger curve yields $\mu_g = 0.45$, $E_{eff} = 1.26$ eV and $s_{eff} = 4.1 \times 10^{16}$ s^{-1}, and the RW curve has $\mu_g = 0.424$, $E_{eff} = 0.83$ eV and $s_{eff} = 4.8 \times 10^{10}$ s^{-1}.

4. Discussion

As pointed out above, the symmetry factor of $\mu_g = 0.56$, found in the "pure" Auger recombination case is characteristic of third-order kinetics peaks. In the literature, there are several reports on TL peaks with high symmetry factors, up to $\mu_g \sim 0.59$. For example, Singh and Singh (2009) reported on TL in γ-irradiated green calcite which yielded high μ_g values up to 0.57. Dubey et al. (2014) described the effect of Eu^{3+} on the TL of $Y_4Al_2O_9$ which yielded different values of μ_g, up to 0.58, depending on the dopant concentration. Tiwari et al. (2014) communicated on TL in $CaZrO_3$:Eu^{3+} in which values of μ_g between 0.55 and 0.58 were found. Chandra et al. (2016) reported on TL in ZnS nanoparticles; values of μ_g between 0.54 and 0.59 were observed. It should be noted, however, that these authors have not attempted to deconvolute their peaks and it is possible that in some of them, the high value of μ_g is actually the result of the occurrence of overlapping components (for an example where such deconvolution has been performed see e.g. Chithambo et al. (2017)).

A point should be made about the determined value of the activation energy which yielded values ~12% lower than the expected 2E, where E is the value inserted in the simulations. The peak-shape method used (Chen, 1969) was developed for peaks with effective order up to 2.5 only. The peaks reported here are of third order in the approximate presentation, and very similar-shaped peaks in the numerical simulations. Therefore, the peak-shape formula cannot be expected to be very accurate, and a discrepancy of ~12% is quite reasonable. Also is interesting the exceedingly high value of the frequency factor s_{eff} which is ~9 orders of magnitude larger than the value entered into the simulations. Obviously, this very high value is associated with the fact that the effective activation energy is so high. In order for a peak with such large activation energy to occur at a relatively low temperature, a very high frequency factor is to be presumed. It is obvious however, that such a high evaluated effective frequency factor of ~10^{22} s^{-1} does not represent the real physical frequency factor which is ~10^{13} s^{-1} in the present case. It should be noted that such high effective frequency factors have been reported in the literature. Several authors reported on high activation energies and very high s values in peak 5 in LiF:Mg, Ti (TLD-100). Taylor and Lilley (1978) communicated on an activation energy of 2.06 eV and a frequency factor of 2×10^{20} s^{-1}. Gorbics et al. (1967) reported $E = 2.4$ eV and $s = 1.7 \cdot 10^{24}$ s^{-1} and Pohlit (1969) reported the exceedingly high values of $E = 3.62$ eV and $s = 10^{42}$ s^{-1}. Ziniker et al. (1973) also described very high values of these parameters in TLD-100. Similar high values were reported in LiF:Mg,Cu,P by Bilski et al. (2008). Such high values of E and s have also been found in other materials. Fartode and Dhoble (2015) measured $s \sim 10^{24}$ s^{-1} in $Ba_3Si_6O_{12}N_2$:Eu^{2+}, and Mandowska et al. (2017) reported on

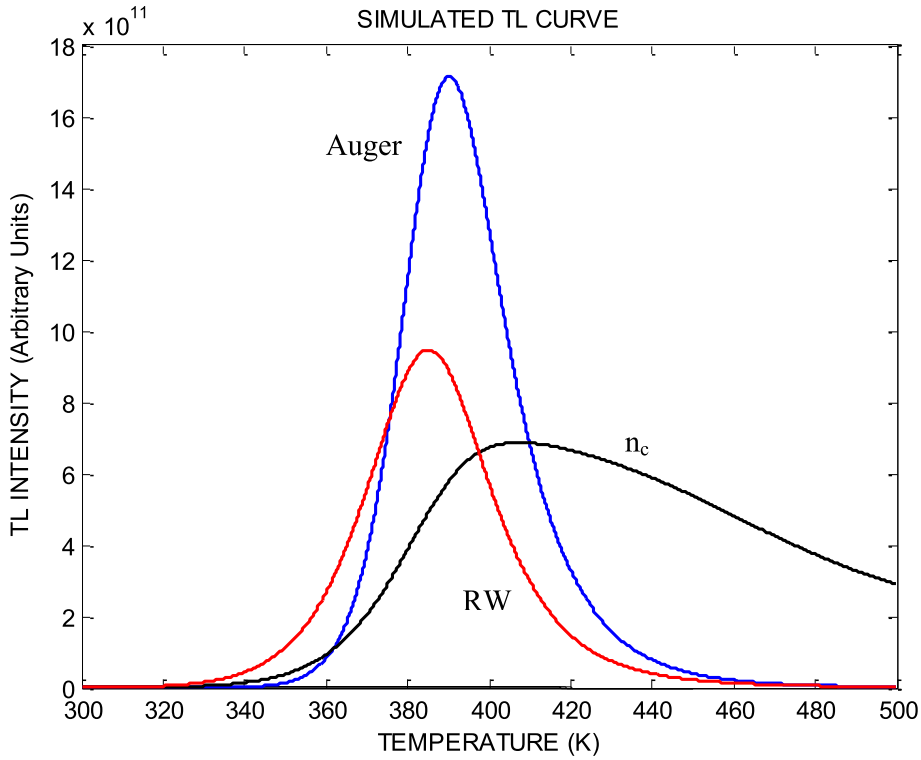

Fig. 5. Auger-recombination peak and RW peak found by the solution of Eqs. (14-16) OTOR model with significant retrapping. The parameters are given in the text. The simulated curve of n_c(T) is also shown.

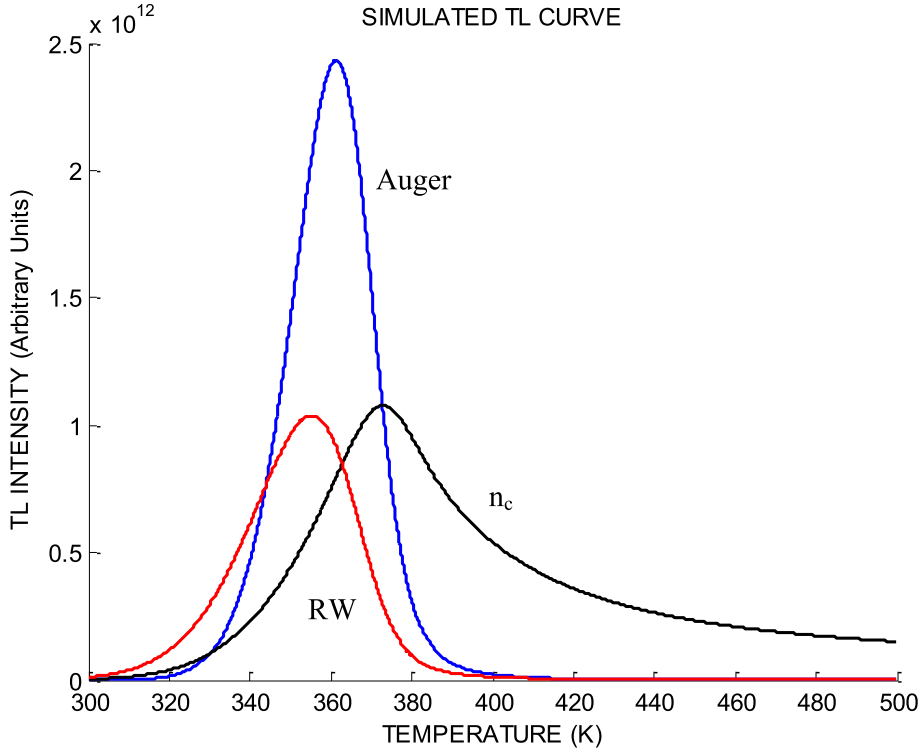

Fig. 6. Auger-recombination peak and RW peak found by the solution of Eqs. (14-16) OTOR model with small retrapping. The parameters are given in the text. The simulated curve of n_c(T) is also shown.

$E = 2.62$ eV and $s \sim 10^{25}$ s^{-1} in KCl crystals. It should be noted that Chen and Hag-Yahya (1996) have given a possible theoretical explanation to these very high values of the parameters by assuming a strong center competition during the process. Mandowski (2005) suggested another explanation based on the semi-localized model for TL. Of course, the present Auger recombination is another possible explanation of these rather anomalous results.

The occurrence of the third power dependence on the dose in the

two-trap one-center case is of interest. The fact mentioned above that the occupancies of the traps n_1 and n_2 and the center m are linear with the dose indicates that the main effect of superlinearity has to do with the process taking place during the heating stage. Probably it is associated with the term mn_c^2 in Eqs. (11) and (12) (see also the Appendix below). This kind of very strong superlinearity, ~3rd power of the dose, has been reported in the literature. Halperin and Chen (1966) described this kind of strong superlinearity as of the very lowest doses in a TL peak occurring at ~250 K in UV irradiated semiconducting diamonds. Chen et al. (1988) reported on a similar effect of ~3rd power dose dependence in a TL peak observed at 110 °C in β-irradiated synthetic quartz. Yet another third-power dose dependence has been communicated by Otaki et al. (1994) in TL from UV-irradiated CaF_2:Tb_4O_7. It should be noted that dose dependence stronger than quadratic has been explained by Chen and Fogel (1993) by using a model which considers competition between traps in both the excitation and heating. The main difference is that in their simulations, the initial dose dependence was found to be quadratic and only at higher doses, the dose dependence became steeper whereas in the present Auger recombination model, the cubic dose dependence is as of the lowest doses, similar to the mentioned experimental results.

Also is of interest the point that, as opposed to the case of one-trap one-center with Auger recombination where approximately third-order kinetics is expected, at least at the low-dose range, in the case where competition with a disconnected trap is considered, the shape of the TL peak is like a first-order curve. This point is commensurate with previous reports to the effect that in the presence of a deep trapping competitor, the TL peak tends to look like a first-order curve nearly irrespective of the trapping parameters (see e.g. Chen and Pagonis, 2013).

In the cases where both Auger and RW-like recombinations are allowed simultaneously (Figs. 5 and 6), the features of the two peaks look closer to first-order when the retrapping probability is small, in similarity to the OTOR RW situation. Still, the symmetry factor is larger with the Auger component than with the RW one, and the effective activation energy and frequency factor are larger than their RW counterparts. In most cases, the emissions of these two kinds of recombination may be measured together yielding some combination peak with intermediate properties. It should be noted however that different relations between the recombination probability coefficients A_a and A may yield TL peaks close to the pure regular OTOR peak or closer to the pure Auger-recombination peak.

It is worth mentioning that as seen in Figs. 5 and 6, the two TL maxima precede that of the peak of $n_c(T)$, this in agreement with the point made about the general occurrence of TL peaks at lower temperature than their thermally stimulated conductivity (TSC) counterparts (see e.g., Chen, 1971).

Appendix

Let us consider the dose dependence of TL for the case of Auger recombination with a competing trap, under some simplifying assumptions. We start with Eqs. (9)-(13). Let us assume, in addition:

1. During irradiation, temperature is low enough so that thermal excitation is negligible for both traps and during heating, thermal excitation occurs first from n_1 and later from n_2. Consequently, during thermal excitation of n_1, which is the trap of interest here, terms involving $s_2\exp(-E_2/kT)$ can be ignored.
2. The dose is low so that $n_1 << N_1$ and $n_2 << N_2$.
3. The free-electron lifetime is short compared to either the characteristic times for irradiation or thermal excitation.
4. Consistent with the low-dose assumption, we will assume that retrapping of free electrons into n_1 and n_2 is stronger than recombination with the center: $A_a n_c^2 << (A_1N_1 + A_2N_2)n_c$.

Under these assumptions, the usual quasi-steady approximation is valid and the free electron and free hole densities become

$$n_c = \frac{X + n_1 s_1 \exp(-E_1/kT)}{A_1N_1 + A_2N_2}, \tag{A1}$$

$$n_v = \frac{X}{B(M - m)}. \tag{A2}$$

It follows that the conservation equations for n_1, n_2 and m reduce to

$$\frac{dn_1}{dt} = \frac{A_1N_1X - A_2N_2n_1s_1 \exp(-E_1/kT)}{A_1N_1 + A_2N_2}, \tag{A3}$$

$$\frac{dn_2}{dt} = \frac{A_2N_2}{A_1N_1 + A_2N_2}[X + n_1s_1 \exp(-E_1/kT)], \tag{A4}$$

$$\frac{dm}{dt} = X - \frac{A_a m}{(A_1N_1 + A_2N_2)^2}[X + n_1s_1 \exp(-E_1/kT)]^2. \tag{A5}$$

We will assume that before irradiation, all trap and center populations are zero, $n_1 = n_2 = m = 0$. We will also assume that irradiation takes place slowly enough that terms involving X^2 are negligible compared to terms involving X. As stated previously, we assume that thermal excitation during irradiation is negligible. It follows that Eqs. (A3)-(A5) can be immediately integrated to find the populations after irradiation,

$$n_{1,0} = \frac{A_1N_1}{A_1N_1 + A_2N_2}D, \tag{A6}$$

$$n_{2,0} = \frac{A_2N_2}{A_1N_1 + A_2N_2}D, \tag{A7}$$

$$m_0 = D, \tag{A8}$$

where the subscript 0 is used to denote the values after irradiation completes and before thermal excitation begins.

The cubic dependence on dose occurs when $A_1N_1 << A_2N_2$. In this case, Eq. (A3) with $X = 0$ reduces to

$$\frac{dn_1}{dt} = -s_1 n_1 exp(-E_1/kT). \tag{A9}$$

During heating, we will assume the usual linear temperature profile: $T = T_0 + \beta t$. During irradiation, we assumed that the temperature was low enough that thermal excitation of the traps could be neglected. Consistent with that, we can assume that T_0 is low enough to neglect here. Integrating Eq. (A9) over time yields

$$n_1(t) = n_{1,0} \exp\left[-\frac{Es}{k\beta}\Gamma(-1, E/kT)\right] \tag{A10}$$

where $\Gamma(-1,E/kT)$ is the incomplete gamma function as defined by Abramowitz and Stegun (1970).

$$\Gamma(a, x) = \int_x^\infty e^{-z} z^{a-1} dz. \tag{A11}$$

From Eq. (A5), the intensity due to recombination at the center is given by

$$I = -\frac{dm}{dt} = \frac{A_a s^2}{(A_1 N_1 + A_2 N_2)^2} m n_1^2 \exp(-2E/kT). \tag{A12}$$

From Eqs. (A6) and (A8) we see that $A_1 N_1 << A_2 N_2$ also leads to $n_1 << m$. Consequently, during the filling of n_1, change in the concentration of m will be negligible. Thus, in Eq. (A12), we can set $m \approx m_0$. Then, substituting Eq. (A10) into Eq. (A12), we find

$$I = \frac{A_a s^2}{(A_1 N_1 + A_2 N_2)^2} m_0 n_{1,0}^2 \exp\left[-\frac{2Es}{k\beta}\Gamma(-1, E/kT)\right] \exp(-2E/kT). \tag{A13}$$

It is clear from Eq. (A13) that the initial rise of the intensity corresponds to a trap energy of $2E$. Also, note the factor $m_0 {n_{1,0}}^2$. Since Eqs. (A6) and (A8) show that $n_{1,0}$ and m_0 each scales linearly in dose D, the factor $m_0 {n_{1,0}}^2$ scales as dose cubed. This explains the cubic dependence on dose depicted in Fig. 3.

References

Abramowitz, M., Stegun, I.A., 1970. Handbook of Mathematical Functions. U.S. Government Printing Office.

Auston, D.H., Shank, C.V., LeFur, P., 1975. Picosecond optical measurements of band-to-band Auger recombination of high-density plasmas in germanium. Phys. Rev. Lett. 35, 1022–1025.

Aytac, Y., Olson, B.V., Kim, J.K., Shaner, E.A., Hawkins, S.D., Klem, J.F., Olesberg, J., Flatté, M.E., Boggess, T.F., 2016. Bandgap and temperature dependence of Auger recombination in InAs/InAsSb type-II superlattices. J. Appl. Phys. 119 (1–4), 215705.

Baird, J.K., 1999. A generalized statement of the law of mass action. J. Chem. Educ. 76, 1146–1150.

Benz, G., Conradt, R., 1977. Auger recombination in GaAs and GaSb. Phys. Rev. B16, 843–855.

Bilski, P., Obryk, B., Olko, P., Mandowska, E., Mandowski, A., Kim, J.L., 2008. Characteristics of LiF:Mg,Cu,P thermoluminescence at ultra-high dose range. Radiat. Meas. 43, 315–318.

Böhm, M., Scharmann, A., 1993. In: Oberhofer, M., Scharmann, A. (Eds.), Theory. *Applied Thermoluminescence Dosimetry*. Adam Hilger Ltd., Bristol, pp. 11–38.

Chandra, B.P., Chandrakar, R.K., Chandra, V.K., Baghel, R.N., 2016. Effect of particle size on activation energy and peak temperature of the thermoluminescence glow curve of undoped ZnS nanoparticles. Luminescence 31, 478–486.

Chen, R., 1969. On the calculation of activation energies and frequency factors from glow curves. J. Appl. Phys. 40, 570–585.

Chen, R., 1971. Simultaneous measurement of thermally stimulated conductivity and thermoluminescence. J. Appl. Phys. 42, 5899–5901.

Chen, R., Fogel, G., 1993. Superlinearity in thermoluminescence revisited. Radiat. Protect. Dosim. 47, 23–26.

Chen, R., Hag-Yahya, A., 1996. Interpretation of very high activation energies and frequency factors in TL as being due to competition between centres. Radiat. Protect. Dosim. 65, 17–20.

Chen, R., Pagonis, V., 2013. On the expected order of kinetics in a series of thermoluminescence (TL) and thermally stimulated conductivity (TSC) peaks. Nucl. Instrum. Methods Phys. Res. B312, 60–69.

Chen, R., Yang, X.H., McKeever, S.W.S., 1988. The strongly superlinear dose dependence of thermoluminescence in synthetic quartz. J. Phys. D Appl. Phys. 21, 1452–1457.

Chithambo, M.L., Wako, A.H., Finch, A.A., 2017. Thermoluminescence of $SrAl_2O_4$:Eu^{2+},Dy^{3+}: kinetic analysis of a composite peak. Radiat. Meas. 97, 1–13.

Dubey, V., Agrawal, S., Kaur, J., 2014. Effect of Eu^{3+} concentration on luminescence studies of $Y_4Al_2O_9$ phosphor. Ind. J. Mater. Sci. 2014, 8.

Fartode, S.A., Dhoble, S.J., 2015. Synthesis and characterization of $Ba_3Si_6O_{12}N_2$:Eu^{2+}. Luminescence 31, 295–304.

Ferner, R.E., Aronson, J.K., 2016. Cato Guldberg and Peter Waage, the history of the law of mass action, and its relevance to clinical pharmacology. Br. J. Clin. Pharmacol. 81, 51–55.

Ghanassi, M., Schave-Klein, M.C., Hache, F., Ekimov, A.I., Ricard, D., Flyzanis, C., 1993. Time-resolved measurements of carrier recombination in experimental semiconductor-doped glasses: confirmation of the Auger recombination. Appl. Phys. Lett. 62, 78–80.

Gorbics, S.G., Attix, F.H., Pfaff, J.A., 1967. Temperature stability of CaF_2:Mn and LiF (TLD-100) thermoluminescent dosimeters. Int. J. Appl. Radiat. 18, 625–630.

Guldberg, C.M., Waage, P., 1864. Etudes sur les affinités. Les Mondes 12, 107–113.

Halperin, A., Chen, R., 1966. Thermoluminescence of semiconducting diamonds. Phys. Rev. 148, 839–845.

Hinkley, S.W., Tsokos, C.P., 1974. A stochastic model for chemical equilibrium. Math. Biosci. 21, 85–102.

Lund, E.W., 1965. Guldberg and Waage and the law of mass action. J. Chem. Educ. 42, 548–550.

Mandowska, E., Majgier, R., Mandowski, A., 2017. Spectrally resolved thermoluminescence of pure potassium chloride crystals. Appl. Radiat. Isot. 129, 171–179.

Mandowski, A., 2005. Semi-localized transitions model for thermoluminescence. J. Phys. D Appl. Phys. 38, 17–21.

McKeever, S.W.S., 1985. Thermoluminescence of Solids. Cambridge University Press, Cambridge.

Oster, L., Haddad, J., 2003. Kinetic analysis of relaxation electron emission: exotic cases of the energy transfer. Mater. Sci. 9 2003; ISSN 1392-1320.

Otaki, H., Kido, H., Hiratsuka, A., Fukuda, Y., Takeuchi, N., 1994. Estimation of UV radiation dose using CaF_2:Tb_4O_7 as a thermoluminescence dosimeter. J. Mater. Sci. Lett. 13, 1267–1269.

Pilkuhn, M.H., 1979. Non-radiative recombination and luminescence in silicon. J. Lumin. 18/19, 81–87.

Pohlit, W., 1969. Thermoluminescence in LiF. I. Measurement of activation energy of electrons in different traps. Biophysik 5, 341–350.

Scharmann, A., Böhm, M., 1993. Basic concepts of thermoluminescence, 1993. In: Oberhofer, M., Scharmann, A. (Eds.), Techniques and Management of Thermoluminescence Dosimetry. Kluwer, Dordrecht, pp. 21–40.

Sheinkman, M.K., 1964. On a possible recombination mechanism at multicharged centers in semiconductors. Sov. Phys. Solid State 5, 2035–2038.

Singh, T.W., Singh, S.D., 2009. Kinetic parameters of thermoluminescence glow curves of γ-irradiated green calcite. Indian J. Pure Appl. Phys. 47, 409–412.

Taylor, G.C., Lilley, E., 1978. The analysis of thermoluminescence glow peaks in LiF (TLD-100). J. Phys. D Appl. Phys. 11 567-501.

Tiwari, N., Kuraria, R.K., Kuraria, S.R., 2014. Thermoluminescence (TL) glow curve and kinetic of $CaZrO_3$:Eu^{3+} phosphor. Adv. Phys. Lett. 1, 15–18.

Tolpygo, E.I., Tolpygo, K.B., Sheinkman, M.K., 1965. Auger recombination involving carriers located at different centers. Sov. Phys. Solid State 7, 1442–1445.

Tolpygo, E.I., Tolpygo, K.B., Sheinkman, M.K., 1974. Nonradiative Auger recombination of electrons at donor-acceptor pairs. Sov. Phys. Semiconduct. 8, 326–328.

Tuan, B.T., Velick ý, B., Bohun, A., 1972. The role of Auger effect in thermostimulated phenomena in ionic crystals. Z. Phys. 251, 289–299.

Vorobev, YuV., Tolpygo, E.I., Sheinkman, M.K., 1984. The Auger process with energy transfer to the bound charge carriers in multi-valley semiconductors. Phys. Status Solidi 123, 295–308.

Ziniker, W.M., Rusin, J.M., Stoebe, T.G., 1973. Thermoluminescence and activation energies in Al_2O_3, MgO and LiF (TLD-100). J. Mater. Sci. 8, 407–414.

Łożykowski, H.J., Oczkowski, H.L., Firszt, F., 1975. Electroluminescence of ZnSe-ZnTe diodes obtained by liquid-phase epitaxy. J. Lumin. 11, 75–81 1975.